

Original Article

# Inhibitory effects of phytochemicals on metabolic capabilities of CYP2D6\*1 and CYP2D6\*10 using cell-based models *in vitro*

Qiang QU<sup>1,2</sup>, Jian QU<sup>1</sup>, Lu HAN<sup>2</sup>, Min ZHAN<sup>1</sup>, Lan-xiang WU<sup>3</sup>, Yi-wen ZHANG<sup>1</sup>, Wei ZHANG<sup>1</sup>, Hong-hao ZHOU<sup>1,\*</sup>

<sup>1</sup>Institute of Clinical Pharmacology, Hunan Key Laboratory of Pharmacogenetics, Xiangya Hospital, Central South University, Changsha 410078, China; <sup>2</sup>Xiangya Hospital, Central South University, Changsha 410008, China; <sup>3</sup>Institute of Life Sciences, Chongqing Medical University, Chongqing 400016, China

**Aim:** Herbal products have been widely used, and the safety of herb-drug interactions has aroused intensive concerns. This study aimed to investigate the effects of phytochemicals on the catalytic activities of human CYP2D6\*1 and CYP2D6\*10 *in vitro*.

**Methods:** HepG2 cells were stably transfected with CYP2D6\*1 and CYP2D6\*10 expression vectors. The metabolic kinetics of the enzymes was studied using HPLC and fluorimetry.

**Results:** HepG2-CYP2D6\*1 and HepG2-CYP2D6\*10 cell lines were successfully constructed. Among the 63 phytochemicals screened, 6 compounds, including coptisine sulfate, bilobalide, schizandrin B, luteolin, schizandrin A and puerarin, at 100  $\mu\text{mol/L}$  inhibited CYP2D6\*1- and CYP2D6\*10-mediated O-demethylation of a coumarin compound AMMC by more than 50%. Furthermore, the inhibition by these compounds was dose-dependent. Eadie-Hofstee plots demonstrated that these compounds competitively inhibited CYP2D6\*1 and CYP2D6\*10. However, their  $K_i$  values for CYP2D6\*1 and CYP2D6\*10 were very close, suggesting that genotype-dependent herb-drug inhibition was similar between the two variants.

**Conclusion:** Six phytochemicals inhibit CYP2D6\*1 and CYP2D6\*10-mediated catalytic activities in a dose-dependent manner *in vitro*. Thus herbal products containing these phytochemicals may inhibit the *in vivo* metabolism of co-administered drugs whose primary route of elimination is CYP2D6.

**Keywords:** CYP2D6; drug interaction; herbal medicine; coptisine; bilobalide; schizandrin; luteolin; puerarin

Acta Pharmacologica Sinica (2014) 35: 685–696; doi: 10.1038/aps.2013.202

## Introduction

Human cytochrome P450 2D6 (CYP2D6) is an extensively characterized polymorphic drug-metabolizing enzyme that catalyzes the bio-conversion of many xenobiotics. CYP2D6 metabolizes more than 25% of drugs, including antidepressants, antipsychotics, beta-receptor antagonists, analgesics, antiarrhythmics, *etc*.<sup>[1,2]</sup> CYP2D6 possesses more than 70 significant alleles, leading to various catalytic activities<sup>[3]</sup>. Compared to the two alleles of 188C and 4268G in CYP2D6\*1 (wild type), CYP2D6\*10 has two single nucleotide polymorphisms (SNP) 188T (rs1065852, Pro34Ser) and 4268C (rs1135840, Ser486Thr) (<http://www.cypalleles.ki.se/cyp2d6.htm>), and the frequencies are 38%–70% in Asians<sup>[4]</sup>. The decreased clearance of drugs *in vivo* by CYP2D6\*10 is caused by low expression

and also increased  $K_m$ <sup>[5]</sup>.

As combination therapy using herbal products with prescription medications becomes more widely used in the world, the safety of herb-drug interactions, especially the inhibition of P450-mediated drug metabolism by herb products, has aroused intense concerns<sup>[6]</sup>. The CYP2D6 catalytic activity is possibly decreased as a result of enzyme inhibition by herbal supplements, including piper nigrum fruit, melaleuca leucadendron leaf<sup>[7]</sup>, goldenseal, valerian<sup>[8]</sup>, black cohosh<sup>[8]</sup>, and naturally occurring compounds, such as eupatorin<sup>[9]</sup>, epiberberine<sup>[10]</sup>, berberine, and hydrastine<sup>[11]</sup>. In recent years, substantial progress has been made in predicting herb-drug interactions, but the presence of polymorphic variants of P450s complicates the prediction. CYP2D6 genotype-dependent herb-drug interactions have been rarely investigated.

HepG2 cells are derived from human hepatoma and show many liver-specific functions. Because of the presence of membrane barriers, transport processes and the NADPH sys-

\* To whom correspondence should be addressed.

E-mail honghaozhou2012@gmail.com

Received 2013-10-03 Accepted 2013-11-11

tem, HepG2 cells closely reflect the *in vivo* situation and are more predictive than microsomes in some aspects<sup>[12]</sup>. However, HepG2 cells lack almost all CYP450s. HepG2 cells transiently or stably transfected with CYP2D6 expression vectors have been used to investigate the metabolism and toxicity of chemicals, as well as to screen drug candidates<sup>[13–15]</sup>. The fluorogenic probe 3-[2-(*N,N*-diethyl-*N*-methyl-ammonium)ethyl]-7-methoxy-4-methylcoumarin (AMMC) is a useful substrate to examine the CYP2D6 activity in transfected-HepG2 cells and rat and human CYP2D6 microsomes<sup>[14,16]</sup>. CYP2D6 *O*-demethylates AMMC to form AMHC (3-[2-(*N,N*-diethyl-*N*-methyl-ammonium)ethyl]-7-hydroxy-4-methylcoumarin), which can be detected by fluorimetry. Thus, our screening model used stably transfected HepG2 cells expressing CYP2D6\*1 or \*10 and quantified CYP2D6 activity by analyzing the conversion of AMMC to AMHC by fluorimetry.

The aims of the present study were to screen phytochemicals to determine whether they inhibit CYP2D6 and to understand the effects of these phytochemicals on the catalytic activities of the CYP2D6 allelic variants, CYP2D6\*1 and \*10. The investigation of genotype-enzyme kinetics and genotype-dependent herb-drug interactions may be important for drug discovery and development, as well as the optimization of drug dosage among individuals, thereby guiding individual therapy.

## Materials and methods

### Chemicals and reagents

AMMC was purchased from BD Gentest (Woburn, MA, USA). DMSO, quinidine, bufuralol, ketoconazole, amiodarone, chlorpromazine, verapamil, cimetidine, quercetin, omeprazole and lovastatin were purchased from Sigma-Aldrich (St Louis, MO, USA). Sixty-three phytochemicals were obtained from Sigma-Aldrich or the National Institutes for Food and Drug Control (Beijing, China). Aminoglycoside antibiotic G418 was purchased from Invitrogen (Carlsbad, CA, USA). All reagents were of high-performance liquid chromatography (HPLC) grade.

### Construction of CYP2D6\*1 and CYP2D6\*10 expression plasmids

Total RNA was extracted from a surgical specimen of the human liver at the Xiangya Hospital using TRIzol reagent (Invitrogen), and the first-strand cDNA was synthesized using a cDNA Synthesis Kit (Takara, Dalian, China). The CYP2D6 cDNA was amplified using primers according to the NCBI Reference Sequence (NM\_000106.4) (Supplementary Table 1)

and then inserted into pcDNA3.1(-) (Invitrogen) in the presence of T4 DNA ligase. Substitutions (188T and 4268C) were introduced into the pcDNA3.1-CYP2D6\*1 vector using the QuikChange Site-directed Mutagenesis Kit (Stratagene, Shanghai, China). The mutation primers are listed in Supplementary Table 1. The constructs were sequenced to confirm the introduction of these mutations.

### Generation of stable cell lines expressing CYP2D6\*1 and CYP2D6\*10 isoforms

The HepG2 cells (HB-8065, ATCC) were cultured in modified Eagle's medium (MEM, Invitrogen) supplemented with 10% fetal calf serum (Abcam Labs, Cambridge, MA, USA) at 37°C in a humidified atmosphere (5% CO<sub>2</sub>) and transfected with pcDNA3.1-CYP2D6\*1, pcDNA3.1-\*10 or pcDNA3.1(-) plasmids using 10 µL Lipofectamine<sup>TM</sup> 2000 (Invitrogen). Clones were selected for G418 resistance for 12 d and subcultured.

### Quantitative real time PCR and Western blotting

Total RNA was extracted from the stable CYP2D6 expressing cells, and the first-strand cDNA was synthesized. The cDNA was amplified by performing quantitative RT-PCR for 40 cycles using SYBR Green (Bio-rad, Hercules, CA, USA) (for primer sequences see Supplementary Table 1). The relative expression of the CYP2D6 mRNA was normalized to β-actin. The analysis was carried out using the 2<sup>-ΔΔCt</sup> method<sup>[17]</sup>.

The whole cell proteins were extracted using the RIPA protein extraction reagent and separated on an 8% SDS-polyacrylamide gel by electrophoresis. The proteins were transferred to a polyvinylidene difluoride membrane (Millipore, Bedford, MA, USA), which was incubated for 1 h at room temperature with rabbit polyclonal antibodies (1:400 dilution, Abcam Labs) against the CYP2D6 protein. The membranes were washed twice for 10 min and incubated with Dylight 800-labeled antibody (1:7500, KPL Inc, Gaithersburg, MD, USA). The membranes were washed twice and analyzed using the Odyssey Infrared Imaging System (LI-COR Biosciences, Lincoln, NE, USA). The relative expression of CYP2D6 was normalized to β-actin.

### Evaluation of the metabolic kinetics of CYP2D6\*1 and \*10 in expression cell models using HPLC and fluorimetry

Cells that stably expressed either CYP2D6\*1 or \*10 were diluted to 1×10<sup>6</sup> cells/mL and cultured in 96-well plates for 24 h. After being washed twice with PBS, cells were incu-

**Table 1.** Kinetic constants for the CYP2D6\*1 and \*10-mediated metabolic activity.

CYP2D6 isoforms	Substrate	Detection Method	$K_m$ (µmol/L)	$V_{max}^a$ (pmol·min <sup>-1</sup> ·mg <sup>-1</sup> )	CL <sub>int</sub> <sup>b</sup>	CL <sub>int</sub> <sup>c</sup> ratio
CYP2D6*1	AMMC	Fluorimetry	12.45±0.65	42.60±0.74	3.42	
CYP2D6*10	AMMC	Fluorimetry	15.58±1.89 <sup>d</sup>	13.67±0.59 <sup>d</sup>	0.88	25.7%
CYP2D6*1	Bufuralol	HPLC	12.58±0.79	123.0±2.57	9.77	
CYP2D6*10	Bufuralol	HPLC	16.56±1.39 <sup>d</sup>	22.09±0.68 <sup>d</sup>	1.33	13.6%

<sup>a</sup> $K_m$  and  $V_{max}$  results are expressed as mean±SD; <sup>b</sup>CL<sub>int</sub> was calculated by  $V_{max}/K_m$ ; <sup>c</sup>CL<sub>int</sub> ratio was calculated by  $CL_{int} \text{ CYP2D6*10} / *1 \times 100\%$ ; <sup>d</sup> $P < 0.05$ .

bated with 15  $\mu\text{mol/L}$  AMMC in 100  $\mu\text{L}$  incubation buffer (1 mmol/L  $\text{Na}_2\text{HPO}_4$ , 137 mmol/L NaCl, 5 mmol/L KCl, 0.5 mmol/L  $\text{MgCl}_2$ , 2 mmol/L  $\text{CaCl}_2$ , 10 mmol/L glucose, and 10 mmol/L Hepes, pH 7.4) for 30 to 150 min at 37°C. Seventy-five microliters of the supernatant was withdrawn per well and transferred to a new 96-well plate. Twenty-five microliters of the 0.1 mol/L sodium acetate buffer (pH 7.4), inclusive of 15 Fishman units of  $\beta$ -glucuronidase and 12 Roy units of arylsulfatase, was added to each well and incubated for 2 h at 37°C. After 200  $\mu\text{L}$  of the quenching solution (0.25 mol/L Tris in 60% acetonitrile) was added to each well, the plates were centrifuged at 3000 rounds per minute for 10 min. The fluorescent metabolite formation was quantified by a Multiskan Ascent 354 Microplate Reader with excitation (390 nm) and emission filters (460 nm). The total cell protein content was determined using the BCA<sup>TM</sup> protein assay kit (Thermo Scientific, Rockford, IL, USA). The results were presented as picomoles of the fluorescent metabolite formed per minute and per milligram of the total cell protein.

To assess the linearity of metabolite formation rates for CYP2D6\*1 and \*10 from bufuralol, bufuralol was incubated under the conditions described above, after dissolving in DMSO (<0.5%, *v/v*). DMSO (0.1%, *v/v*) was used as the vehicle control. The reactions were terminated by adding 100  $\mu\text{L}$  of acetonitrile, and the samples were centrifuged at 3000 rounds per minute for 10 min. The metabolite 1'-hydroxy bufuralol was quantified by HPLC analysis as described previously<sup>[16]</sup>.

The metabolic kinetics of AMMC and bufuralol catalyzed by CYP2D6\*1 and \*10 were analyzed. AMMC and bufuralol were incubated with HepG2-CYP2D6\*1 or CYP2D6\*10 for 90 min at increasing concentrations (0–80  $\mu\text{mol/L}$ ). The formation of the fluorescent metabolite AMHC and 1'-hydroxy bufuralol were detected as described above.

#### Inhibition constant determination

To detect the effects of potent CYP2D6 inhibitors on CYP2D6-mediated AMMC-O-demethylation, nine different compounds (0–200  $\mu\text{mol/L}$ ) were selected for the inhibition assays. The incubation conditions were the same as the enzyme kinetic assays described above. The compounds were classified as potent ( $\text{IC}_{50}$ <5  $\mu\text{mol/L}$ ), moderate (5  $\mu\text{mol/L}$ < $\text{IC}_{50}$ <50  $\mu\text{mol/L}$ ), poor (50  $\mu\text{mol/L}$ < $\text{IC}_{50}$ <200  $\mu\text{mol/L}$ ), or no inhibition ( $\text{IC}_{50}$ >200  $\mu\text{mol/L}$ ). The inhibition constant ( $K_i$ ) of the prototypical inhibitor quinidine was also determined.

#### Screening inhibition assay

A two-step incubation method was utilized to screen for CYP2D6 inhibitors among the phytochemicals. The initial inhibition assays utilized HepG2-CYP2D6\*1, HepG2-CYP2D6\*10 and control cells at a final density of  $1 \times 10^5$  cells/well in 96-well plates, 100  $\mu\text{mol/L}$  phytochemicals, and 15  $\mu\text{mol/L}$  AMMC in incubation buffer in a total volume of 100  $\mu\text{L}$ . The detection method for detecting the fluorescent metabolites is described above. We selected the inhibitors from the phytochemicals in the initial screen (>50% inhibition rate). To further characterize the inhibition of CYP2D6\*1 and

\*10-mediated AMMC-O-demethylation, the stably transfected cells were incubated with 15  $\mu\text{mol/L}$  AMMC and multiple concentrations of the inhibitors, ranging from 0 to 80  $\mu\text{mol/L}$ . To determine the mode of inhibition, the stably transfected cells were incubated with various concentrations of AMMC (0–80  $\mu\text{mol/L}$ ) and the inhibitors (0.5- and 1-fold of  $\text{IC}_{50}$ ).

#### Statistical analysis

The data are presented as the mean $\pm$ SD of  $n=3$  replicates. The  $\text{IC}_{50}$  values (concentration of phytochemicals that inhibit CYP2D6 activity by 50%) were calculated from the dose-response data using the SPSS 13.0 software (Chicago, IL, USA). The Michaelis constants ( $K_m$ ) and the maximum velocities ( $V_{\text{max}}$ ) for the CYP2D6 catalytic activities were estimated by nonlinear regression analysis using the Michaelis-Menten equation by GraphPad Prism 5 (San Diego, CA, USA). The ratio of  $V_{\text{max}}$  and  $K_m$  was used to calculate the *in vitro* intrinsic clearance ( $\text{CL}_{\text{int}}$ ). In inhibition assays, the data were plotted on an Eadie-Hofstee plot for the visual inspection of the inhibition type, and the  $K_i$  was determined using the global fit for competitive inhibition by GraphPad Prism 5. The statistical analysis was performed using Student's *t*-test (two groups) by SPSS 13.0, and the significant differences were set at  $P<0.05$ .

## Results

#### mRNA and protein expression levels in stably transfected cells

To construct the CYP2D6 expression vector, human CYP2D6\*1 cDNA (wild type) was inserted into pcDNA3.1(-) and verified by sequencing. The mutations of 188T and 4268C were introduced into the wild type cDNA by site-directed mutagenesis and verified by sequencing (Figure 1A). The HepG2 cells were transfected with the control vector (pcDNA3.1), the wild-type vector (CYP2D6\*1) or the mutation vector (CYP2D6\*10). As shown in Figure 1B and 1C, the mRNA and protein levels of CYP2D6\*1 and \*10 in their respective transfected cells were remarkably higher than that in the control cells transfected with pcDNA3.1. We selected those transfected cells which did not show a significant difference between the expression of CYP2D6\*1 and \*10.

#### Enzyme kinetics of CYP2D6\*1 and \*10

AMMC is catalyzed by CYP2D6 to AMHC (Figure 2A), which can be detected by fluorimetry. In Figure 2B, the metabolite 1'-OH bufuralol was detected by HPLC. We detected the linearity of metabolite formation for a duration of 120 min. As shown in Figure 2C, the rates of AMMC-O-demethylation and bufuralol 1'-hydroxylation represent the activity of CYP2D6\*1 and \*10, which are linear with the incubation time. Thus, an incubation time of 90 min was utilized in all subsequent experiments.

The kinetics constants ( $K_m$ ,  $V_{\text{max}}$ , and  $\text{CL}_{\text{int}}$ ) of CYP2D6\*1 and \*10 catalyzing AMMC and bufuralol are presented in Table 1. As shown in Figure 2D and Table 1, compared with CYP2D6\*1, the  $K_m$  estimates for CYP2D6\*10 ( $P<0.05$ ) were 1.25- and 1.32-fold higher for AMMC and bufuralol, respectively. The  $V_{\text{max}}$  values for CYP2D6\*1 were 3.12- and 5.57-

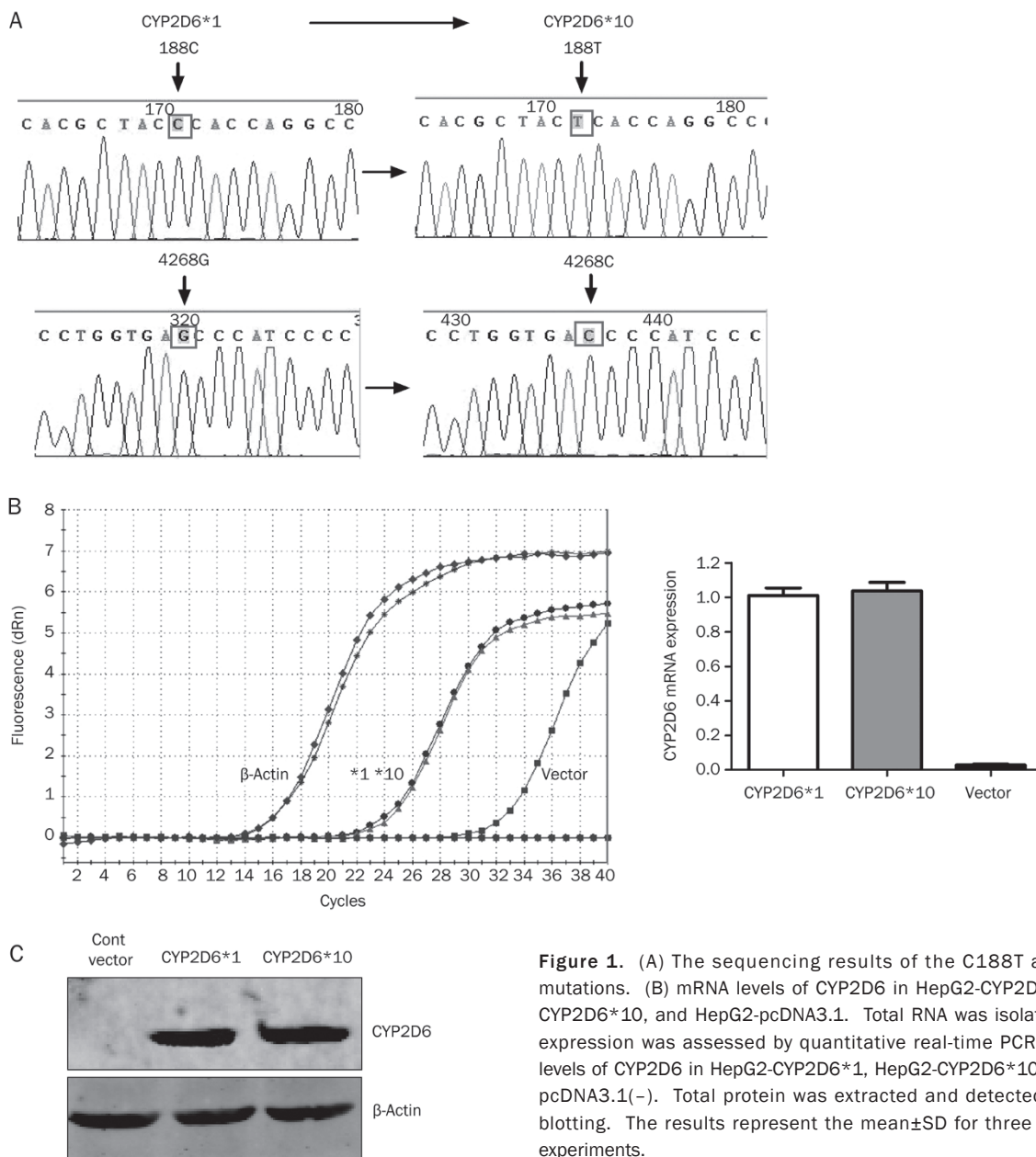


**Figure 1.** (A) The sequencing results of the C188T and G4268C mutations. (B) mRNA levels of CYP2D6 in HepG2-CYP2D6\*1, HepG2-CYP2D6\*10, and HepG2-pcDNA3.1. Total RNA was isolated and gene expression was assessed by quantitative real-time PCR. (C) Protein levels of CYP2D6 in HepG2-CYP2D6\*1, HepG2-CYP2D6\*10, and HepG2-pcDNA3.1(-). Total protein was extracted and detected by Western blotting. The results represent the mean±SD for three independent experiments.

fold higher than those for CYP2D6\*10 ( $P<0.05$ ). CYP2D6\*10 had a lower maximum velocity, resulting in the  $CL_{int}$  values of AMMC and bufuralol metabolites being 25.6% and 13.6% of that of CYP2D6\*1, respectively. A substrate concentration (15  $\mu\text{mol/L}$ ) approximating the apparent  $K_m$  value of AMMC was utilized in all subsequent experiments.

#### Inhibition of CYP2D6\*1 and \*10 activity by quinidine

Quinidine, a well-known inhibitor of CYP2D6, was used as a positive control in the inhibition assay. As shown in Figure 3A, a log-linear decrease in AMMC-*O*-demethylation and bufuralol 1'-hydroxylation was evident at the concentrations of  $1 \times 10^{-3}$  to 100  $\mu\text{mol/L}$ . According to the visual inspection of the Eadie-Hofstee plots (Figure 3B), quinidine competitively inhibited CYP2D6\*1- and \*10-catalyzed AMMC-*O*-demethyl-

ation with  $K_i$  values of 0.012 and 0.038  $\mu\text{mol/L}$ , respectively, as well as bufuralol 1'-hydroxylation with  $K_i$  values of 0.018 and 0.04  $\mu\text{mol/L}$ , respectively. The ratios of the  $K_i$  values of quinidine were 3.315  $\mu\text{mol/L}$  for AMMC and 2.211  $\mu\text{mol/L}$  for bufuralol, showing a higher affinity for CYP2D6\*1 than CYP2D6\*10. As seen in Table 2, the  $IC_{50}$  values of other compounds were determined and classified as potent, moderate, poor, or no inhibition, in accordance with the previous results<sup>[17]</sup>.

In Table 2, we found that most  $IC_{50}$  values of the moderate inhibitors were lower than 100  $\mu\text{mol/L}$ . High concentrations of phytochemicals inhibited the activity of the transfected HepG2 cells, while low concentrations did not (data not shown). Thus, in the next study, we chose 100  $\mu\text{mol/L}$  as the phytochemical concentration.

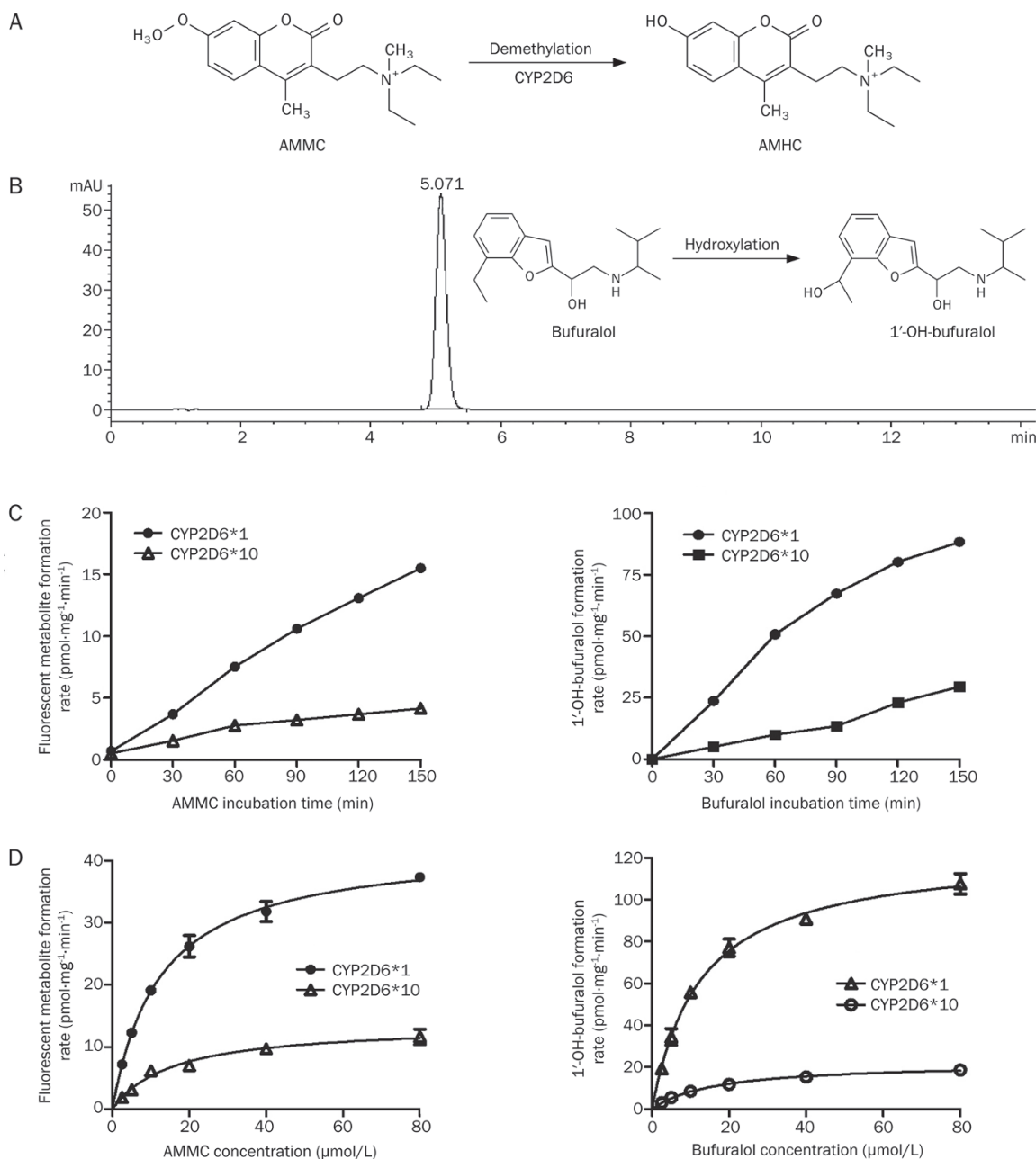


**Figure 2.** (A) Structure of AMMC and the metabolite AMHC. (B) Chromatograms of the standard solution containing 10 ng/mL 1'-OH-bufuralol and structure of AMMC and the metabolite AMHC. (C) Time-dependent metabolism of AMMC by CYP2D6\*1 and \*10. AMMC (15 μmol/L) was incubated with HepG2-CYP2D6\*1 or CYP2D6\*10 in 96-well plates. The values are means±SD of triplicate determinations. (D) The metabolic kinetics of AMMC catalyzed by CYP2D6\*1 and \*10 were analyzed. The metabolic activities of AMMC at increasing concentrations were measured with HepG2-CYP2D6\*1 (closed circles) or CYP2D6\*10 (triangles) in 96-well plates. The values (mean±SD) were fitted to the Michaelis-Menten equation using non-linear regression analysis.

### Screening of potential phytochemical inhibitors

Based on the incubation conditions of 15 μmol/L AMMC at 90 min, a total of 63 phytochemicals (100 μmol/L) were screened using the HepG2-CYP2D6\*1 and \*10 cell models. As shown in Table 3, bilobalide, coptisine sulfate, schizandrin B, and luteolin produced extensive inhibition (inhibition >70%), and schizandrin A and puerarin produced moderate inhibition (70%>inhibition>50%).

### Inhibitory effects of phytochemicals on CYP2D6\*1 and \*10-mediated AMMC-O-demethylation

To further confirm the hits from the initial screen, we investigated the concentration-dependent effects of the phytochemicals on CYP2D6\*1 and \*10-mediated AMMC-O-demethylation. As shown in Figure 4, the potent inhibitors, including bilobalide, coptisine sulfate, schizandrin B, luteolin, schizandrin A, and puerarin, inhibited the catalytic activity of

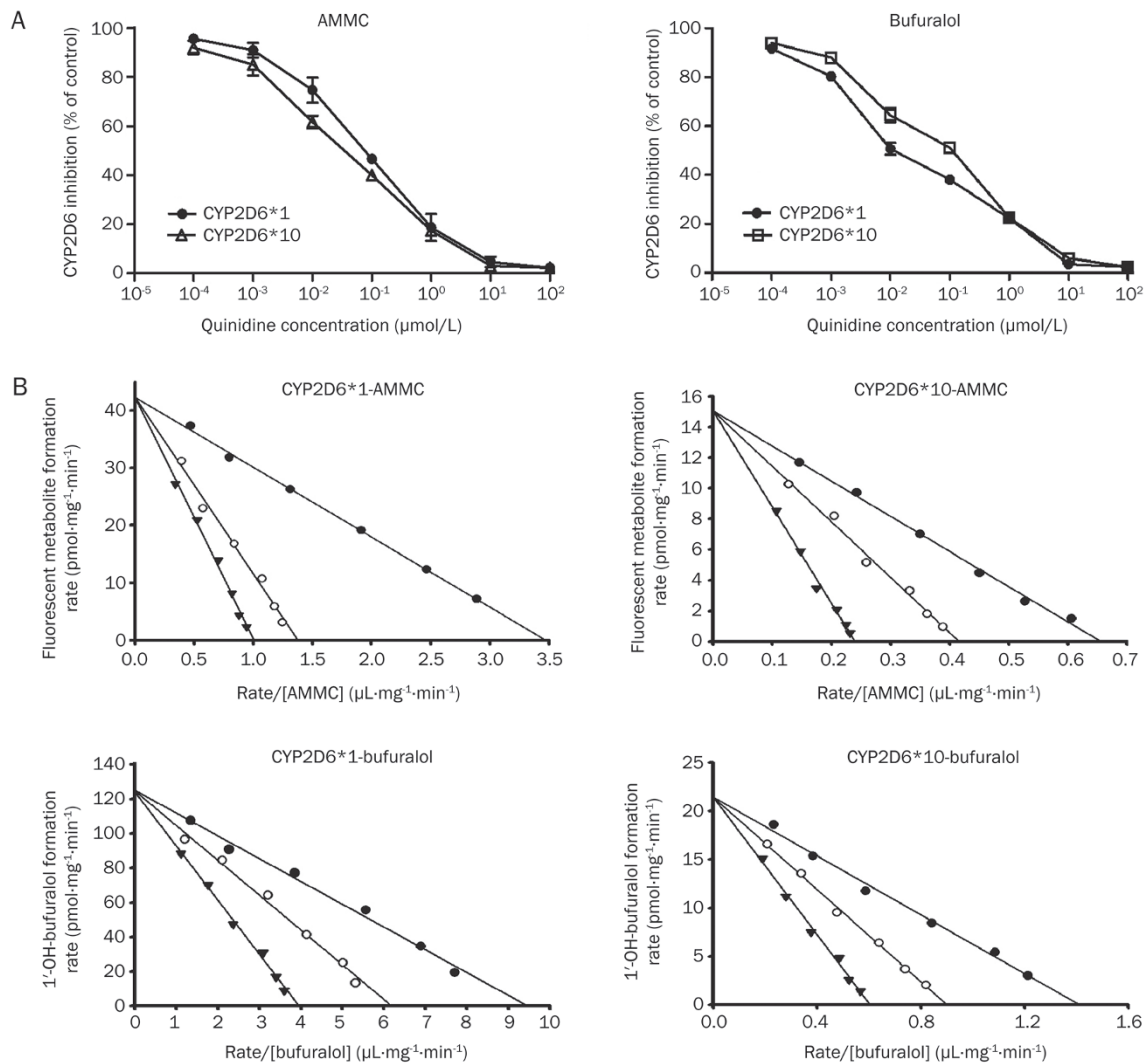


**Figure 3.** (A) Effects of quinidine at different concentrations on CYP2D6\*1 and \*10-mediated AMMC-O-demethylation and bufuralol 1'-hydroxylation. The results are expressed as percentage of control (assayed in the absence of quinidine). (B) Representative Eadie-Hofstee plots for quinidine inhibition of CYP2D6\*1 and \*10-catalyzed AMMC-O-demethylation and bufuralol 1'-hydroxylation. The substrate AMMC concentration ranged from 0 to 80  $\mu\text{mol/L}$ , whereas the quinidine concentrations used were 0  $\mu\text{mol/L}$  ( $\bullet$ ), 0.5-fold of the IC<sub>50</sub> values ( $\circ$ ), and 1-fold of the IC<sub>50</sub> values ( $\blacktriangledown$ ).

**Table 2.** Inhibition of CYP2D6\*1 and \*10 isoforms by several compounds.

Compound	CYP2D6*1		CYP2D6*10	
	IC <sub>50</sub> ( $\mu\text{mol/L}$ ) <sup>a</sup>	Type of inhibitor <sup>b</sup>	IC <sub>50</sub> ( $\mu\text{mol/L}$ ) <sup>a</sup>	Type of inhibitor <sup>b</sup>
Quinidine	0.06±0.02	Potent	0.03±0.01	Potent
Ketoconazole	3.98±0.12	Potent	4.02±0.23	Potent
Amiodarone	9.12±0.23	Moderate	8.89±0.32	Moderate
Chlorpromazine	11.45±0.34	Moderate	12.09±0.29	Moderate
Verapamil	15.12±0.34	Moderate	14.89±0.46	Moderate
Cimetidine	58.99±3.12	Poor	56.23±4.23	Poor
Quercetin	179.21±8.12	Poor	184.34±9.12	Poor
Omeprazole	>200	Noninhibitor	>200	Noninhibitor
Lovastatin	>200	Noninhibitor	>200	Noninhibitor

<sup>a</sup> IC<sub>50</sub> values (concentration of phytochemicals that inhibits CYP2D6 activity by 50%) were calculated from dose-response data using the SPSS 13.0 software;

<sup>b</sup> The compounds were classified as potent (<5  $\mu\text{mol/L}$ ), moderate (from 5 to 50  $\mu\text{mol/L}$ ), poor (from 50 to 200  $\mu\text{mol/L}$ ), or noninhibitor (>200  $\mu\text{mol/L}$ ).

**Table 3.** Inhibition effects of phytochemicals on the CYP2D6\*1 and \*10-mediated AMMC-O-demethylation.

Phytochemicals	CYP2D6*1 inhibition rate <sup>a</sup>	CYP2D6*10 inhibition rate <sup>a</sup>	Phytochemicals	CYP2D6*1 inhibition rate <sup>a</sup>	CYP2D6*10 inhibition rate <sup>a</sup>
AMMC	0.00±0.97	0.00±8.83	Phillyroside	24.30±5.60	24.69±7.77
Quinidine	93.68±0.84	87.65±8.09	Matrine	23.92±10.26	25.62±7.98
Bilobalide	79.92±5.19	80.25±2.33	Cinnamic acid	22.96±4.72	19.44±6.68
Coptisine Sulfate	79.66±5.31	57.10±3.85	Salvianic acid A	23.08±10.34	9.26±5.63
Schizandrin B	76.19±9.80	59.26±12.14	Salvianolic acid B	22.49±5.12	19.14±5.10
Luteolin	74.18±5.00	62.35±4.57	Nobiletin	21.30±1.70	25.93±9.40
Schizandrin A	66.49±2.51	59.26±8.83	Paclitaxel	20.86±7.77	24.38±6.50
Puerarin	64.38±4.43	62.65±3.85	Evodine	20.02±2.76	15.74±6.68
Barbaloin	48.26±7.05	39.20±5.66	Rubescensine a	20.34±7.37	17.28±8.90
Wogonin	47.31±3.64	36.73±8.80	Tanshinone IIA	19.49±7.91	10.49±5.43
Isorhynchophylline	44.05±2.81	37.96±7.91	Caffeic acid	19.60±6.57	6.17±4.57
Huperzine A	43.94±2.73	28.40±7.43	Salidroside	18.23±3.90	16.36±7.43
Ginsenoside Rd	43.52±3.48	50.31±7.48	Breviscapine	18.12±6.99	21.60±6.17
Palmitine HCl	43.62±3.38	35.80±1.41	Oroxin A	18.44±6.03	24.38±10.20
Hyperforin	41.94±1.74	37.04±8.93	Peiminine B	17.78±5.64	24.07±5.63
Hyperoside	42.36±4.21	42.28±3.85	Byakangelicol	17.70±5.59	19.14±6.02
Ginkgolide c	38.36±4.18	33.02±2.83	Picroside II	18.12±6.03	17.28±8.90
Byakangelicin	37.93±2.03	33.64±2.33	Gyenoside XLX	17.07±4.60	10.80±5.95
Resveratrol	36.25±3.48	25.93±10.68	Schisandrin	15.28±4.97	15.12±4.18
Ferulic acid	34.35±4.63	21.60±6.02	Icariin	15.56±8.01	14.20±4.38
Quercitrin	34.04±2.87	37.65±7.87	Ginsenoside Rc	13.80±3.95	21.60±6.17
Echinacoside	31.82±4.94	28.40±5.10	Aloe-emodin	13.38±5.18	9.88±4.38
Dehydroandrograpolid	32.67±4.04	30.25±5.10	Arctiin	12.59±4.46	10.80±5.95
Rutaecarpine	30.87±4.47	29.32±6.50	Aurantio-obtusin	12.86±2.10	14.20±11.05
Astragaloside	31.09±6.01	16.98±10.20	Capsicine	11.30±8.19	9.88±3.74
Oleanolic Acid	29.93±3.55	21.60±6.02	Salvianolic acid	11.30±4.10	16.67±7.91
Imperatorin	29.40±4.27	23.77±3.25	Apigenin	10.56±3.64	11.11±4.81
Cytisine	28.98±9.51	20.68±7.01	Psoralen	9.81±7.58	13.58±3.74
Catharanthine	28.45±5.74	18.52±7.23	Ophiopogonin D	9.07±3.39	4.94±11.05
Cimifugin	27.51±7.86	20.06±6.17	Glabridin	8.89±8.07	5.56±3.34
Prim-O-glucosylcimifugin	26.51±4.78	19.75±6.30	Silymarin	7.23±11.45	19.44±3.70
Magnolol	26.10±2.72	31.48±8.83	Rutin	5.19±2.63	4.01±6.57
Rheinic acid	25.61±4.38	24.38±2.33			

<sup>a</sup> The inhibition rate was measured by  $[1 - (\text{sample data} - \text{blank data}) / (\text{negative control data} - \text{blank data})] \times 100\%$ . The data were expressed as mean ± SD.  $n \geq 3$ .

<sup>b</sup> DMSO (0.1%) in the incubation buffer was used as blanks.

<sup>c</sup> Fluorogenic prober AMMC (15 μmol/L) was used as a negative control.

<sup>d</sup> Quinidine as the positive control.

CYP2D6\*1 and \*10 in a dose-dependent manner. However, the  $IC_{50}$  values for the CYP2D6\*1 and \*10 isoforms inhibited by these potent inhibitors were not different (Table 4). To determine the type of inhibition, the inhibition data were plotted on an Eadie-Hofstee plot. These data demonstrate that all phytochemicals tested competitively inhibit CYP2D6\*1 and \*10 (Figure 5).  $K_i$  values obtained from the CYP2D6\*10 cells were slightly higher than those from the CYP2D6\*1 cells, but the ratios of the  $K_i$  values ( $K_i$  value of CYP2D6\*10/ $K_i$  value of CYP2D6\*1) ranged from 1.05 to 1.30, which are lower than the  $K_i$  ratios for quinidine.

## Discussion

In the present study, we established CYP2D6\*1 and \*10

expressing cell models, and the experimental conditions were optimized for the initial screening of the phytochemical inhibitors. We determined the relative catalytic activities of CYP2D6\*1 and CYP2D6\*10 for metabolizing AMMC and bufuralol and gained an understanding of the effects of the inhibitors on the variants of CYP2D6. In the initial screening study, six phytochemicals competitively inhibited CYP2D6\*1- and \*10-mediated AMMC-O-demethylation in a dose-dependent manner, but the  $K_i$  values for CYP2D6\*1 and \*10 were not different.

Although the inter-individual variation in the metabolic capacity of CYP2D6 and the association with genotype has been investigated<sup>[18]</sup>, CYP2D6 genotype-dependent drug-drug or herb-drug interactions remain less examined. CYP2D6\*10

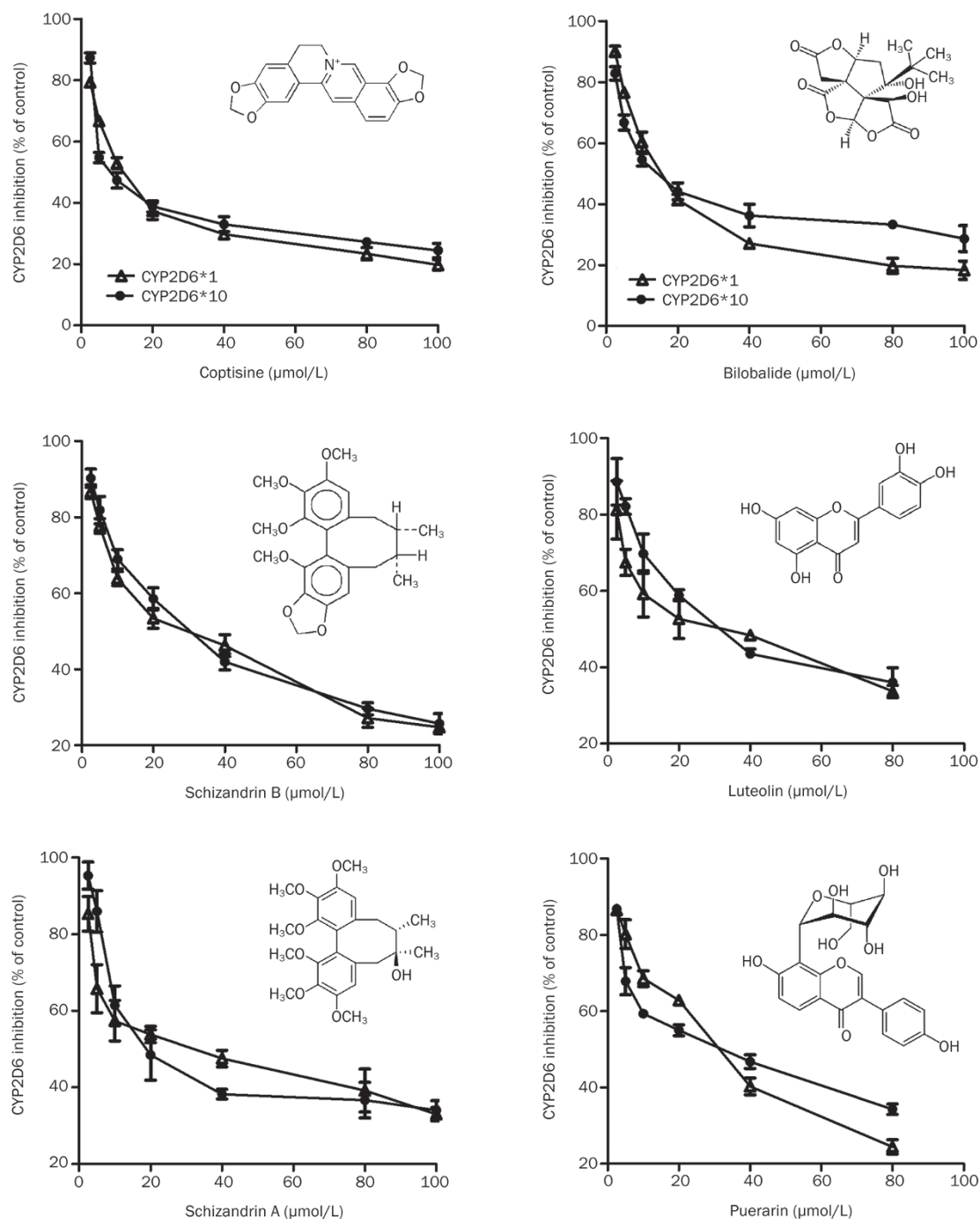


**Figure 4.** Concentration-dependent effects of phytochemicals on CYP2D6\*1 and \*10-mediated AMMC-O-demethylation. HepG2-CYP2D6\*1 (triangles) and \*10 (closed circles) were incubated with various concentrations of the phytochemicals and 12 μmol/L AMMC. The metabolites were detected by fluorimetry as described in the Materials and methods section. AMMC in the absence of phytochemicals (0 μmol/L) was used as the control, HepG2-pcDNA3.1 was used as the blank, and data are represented as the percentage of the control, following the formula: (sample data-blank)/(control data-blank)×100%. The values are presented as the mean±SD of triplicate determinations in a single experiment.

is associated with increased  $K_m$  values for substrates such as bufuralol, venlafaxine, and *p*-tyramine<sup>[5, 19]</sup>. In the present study, we found the expression of CYP2D6\*10 to be different in transfected HepG2 cells. To compare with CYP2D6\*1, we selected cells with an expression of CYP2D6\*10 similar to that of CYP2D6\*1. Thus, we could identify the difference in

inhibition by phytochemicals for CYP2D6\*1 and \*10, which eliminates the complication due to different expressions of CYP2D6\*1 and \*10.

In our studies, the kinetic parameters for the CYP2D6\*10-mediated biotransformation of AMMC and bufuralol were determined, which consistently showed lower catalytic effi-



**Table 4.** Inhibition of AMMC-O-demethylation in CYP2D6\*1 and \*10 by phytochemicals.

Phytochemicals	IC <sub>50</sub> ±SD (μmol/L) <sup>a</sup>		Apparent K <sub>i</sub> <sup>b</sup>		K <sub>i</sub> ratio <sup>c</sup>
	CYP2D6*1	CYP2D6*10	CYP2D6*1	CYP2D6*10	
Coptisine sulfate	12.70±0.87	12.55±0.44	6.38	8.03	1.26
Bilobalide	16.88±0.97	18.28±1.86	12.35	15.84	1.28
Schizandrin B	24.80±0.90	28.33±2.28	13.12	17.08	1.30
Luteolin	25.47±2.90	32.40±2.59	14.10	17.29	1.23
Puerarin	25.96±1.64	26.44±1.23	15.04	15.73	1.05
Schizandrin A	27.77±1.14	29.98±4.55	17.27	19.75	1.14

<sup>a</sup> IC<sub>50</sub> values were generated by several phytochemical inhibitions of CYP2D6\*1 and CYP2D6\*10-catalyzed AMMC-O-demethylation. Results are expressed as mean±SD. n≥3.

<sup>b</sup> Apparent K<sub>i</sub> values were determined using global fit for competitive inhibition.

<sup>c</sup> K<sub>i</sub> ratio was calculated by K<sub>i</sub> values CYP2D6\*10/\*1.

ciencies and lower affinity compared with CYP2D6\*1. Because CYP2D6\*10 exhibited small K<sub>m</sub> changes, the decreased intrinsic clearance for CYP2D6\*10 towards AMMC and bufuralol was mainly due to a substantial decrease in the V<sub>max</sub>. In previous studies, the K<sub>m</sub> values for CYP2D6\*1- and \*10-mediated bufuralol 1'-hydroxylation were in the range of 1.7 to 25 μmol/L and 12 to 50 μmol/L, respectively<sup>[20]</sup>, similar to our results. The K<sub>m</sub> value (12.45 μmol/L) for the CYP2D6\*1 metabolism of AMMC in our studies was lower than the previously reported K<sub>m</sub> value (19.2 μmol/L), which was also determined using cell models<sup>[17]</sup>, but higher than that using human liver microsomes (3 μmol/L)<sup>[14]</sup>. The reason for the variances among these studies might be due to different sources and expression levels of enzyme used, as well as the different incubation conditions used.

To validate the CYP2D6 inhibition assay using AMMC, the concentration-dependent inhibitions and the representative Eadie-Hofstee plots indicated that the positive inhibitor quinidine competitively inhibited CYP2D6\*1- and \*10-mediated AMMC-O-demethylation and bufuralol 1'-hydroxylation. In the initial screening assay, six phytochemicals inhibited CYP2D6\*1 and \*10 in a concentration-dependent manner. Representative Eadie-Hofstee plots for the phytochemicals showed that the mode of inhibition is competitive. K<sub>i</sub> ratios (K<sub>i</sub> values of CYP2D6\*10/\*1) of the phytochemicals ranged from 1.05 to 1.30, indicating that the CYP2D6\*10 inhibition by the phytochemicals is not more pronounced than CYP2D6\*1. Quinidine was found to be a more effective inhibitor of CYP2D6\*1 by K<sub>i</sub> values 2- to 3-fold higher than CYP2D6\*10, which is similar to previous results<sup>[22]</sup>. However, a direct extrapolation that other inhibitors of CYP2D6\*1 have a higher affinity for CYP2D6\*1 than the other variants is not true. Previous studies have found that the enzyme-substrate affinity or enzyme-inhibitor affinity of the functionally reduced allelic variants (CYP2D6\*10 and \*17) can be lower, higher, or comparable to that of CYP2D6\*1<sup>[22]</sup>.

Bilobalide is a major constituent of the terpenoids in *Ginkgo* leaves and produces several neuroprotective effects<sup>[21]</sup>. Bilobalide competitively inhibited the catalytic activity of human recombinant CYP2D6 (IC<sub>50</sub>=11 μmol/L)<sup>[22]</sup>. After a

single oral dose of different *Ginkgo* products such as Geri-force tincture, *Ginkgo* fresh plant extract tablets and EGb 761 tablets, the resulting maximum concentrations of bilobalide in plasma were 3.53, 11.68, and 26.85 ng/mL<sup>[23]</sup>, respectively, less than the IC<sub>50</sub> values from previous studies and our results. However, the bioavailability and pharmacokinetics of *Ginkgo* products for long-term use should be further investigated in clinical trials.

Coptisine is an alkaloid found in the Chinese goldthread (*Coptis chinensis*) and plays an important role in cardioprotection and treating digestive disorders<sup>[24]</sup>. Coptisine displayed a strong concentration-dependent inhibition of CYP2D6 (IC<sub>50</sub>=4.4 μmol/L) using human liver microsomes (HLM)<sup>[10]</sup>. Although bilobalide and coptisine inhibited AMMC-O-demethylation in our studies, the IC<sub>50</sub> values from our stably transfected cell models were higher than those from the recombinant enzyme and HLM. We speculate that the higher IC<sub>50</sub> value may be due to the transportation of the phytochemicals through the HepG2 cell membranes and/or different incubation conditions.

Schizandrin A and schizandrin B are major ingredients of the schizandrin fruit extract, which protects the liver against toxicant challenges<sup>[25, 26]</sup>. It has been reported that schizandrin A and schizandrin B display a competitive inhibition of CYP2D6-dependent activity to a limited extent (IC<sub>50</sub> values >10 μmol/L)<sup>[27, 28]</sup>. In this study, we observed that schizandrin A and schizandrin B competitively inhibited CYP2D6\*1 and \*10 (IC<sub>50</sub>=27.76 and 24.8 μmol/L), respectively.

Luteolin, one of the more common flavones, is a free radical scavenger that plays a role in antioxidation and the modulation of the immune system<sup>[29, 30]</sup>. Reports have found that the CYP2D6-catalyzed dextromethorphan demethylation was reduced to approximately 40% of the control activity when exposed to 50 μmol/L luteolin<sup>[31]</sup>. In the present study, similar results were observed as the CYP2D6\*1-catalyzed AMMC-O-demethylation was reduced to 27.6% by 40 μmol/L luteolin. It was reported that the detectable plasma concentration of luteolin was at most 15 μmol/L after realistic consumption<sup>[32]</sup>. That study indicated that 15 μmol/L luteolin most likely inhibits CYP2D6 activity, but a clinical pharmacology study is

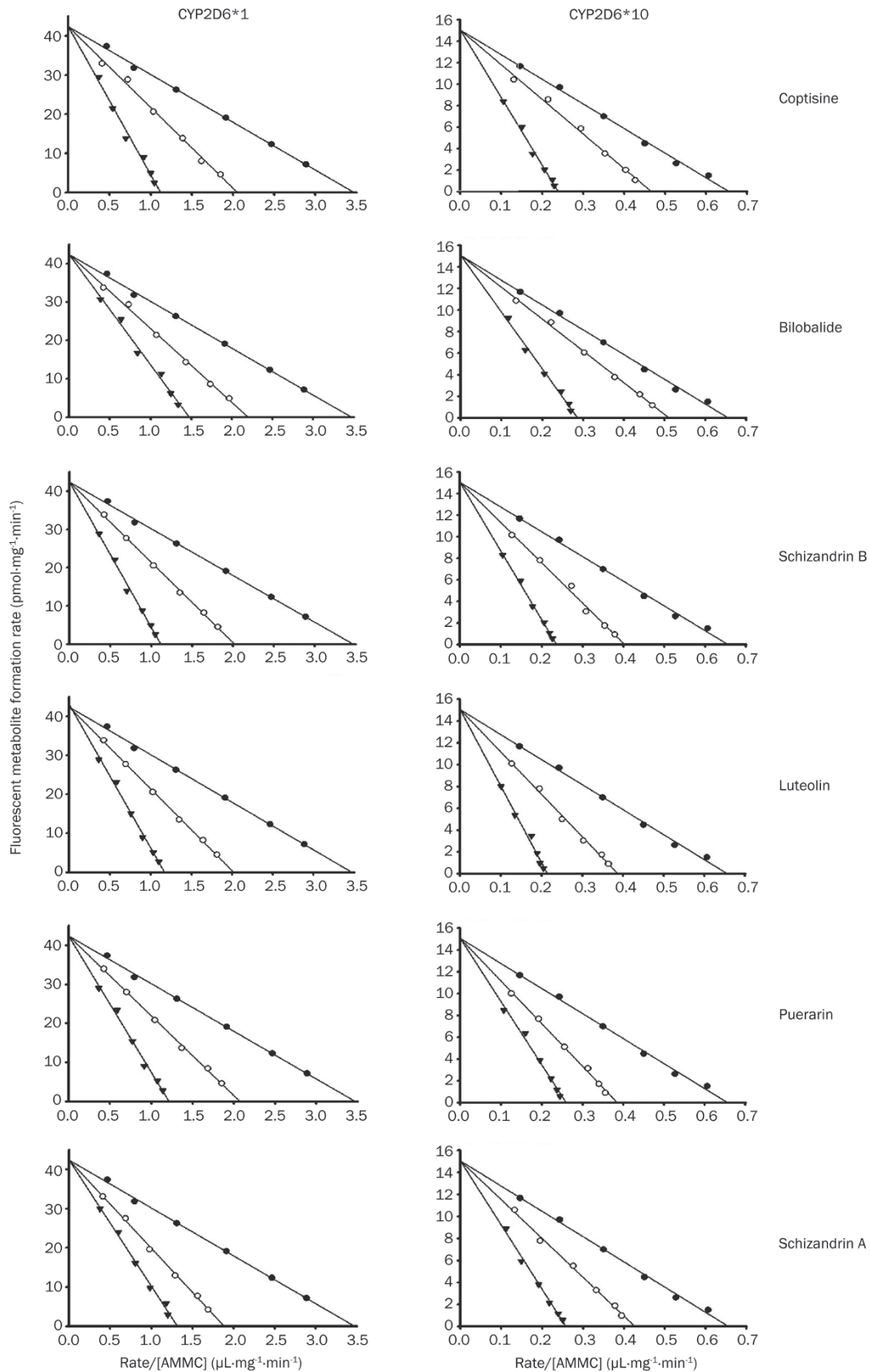


**Figure 5.** Representative Eadie-Hofstee plots for phytochemical inhibition of CYP2D6\*1 and \*10-catalyzed AMMC-O-demethylation. The substrate AMMC concentration ranged from 0 to 80  $\mu\text{mol/L}$ , whereas the inhibitor concentrations used were 0  $\mu\text{mol/L}$  ( $\bullet$ ), 0.5-fold of the  $\text{IC}_{50}$  values ( $\circ$ ) and 1-fold of the  $\text{IC}_{50}$  values ( $\blacktriangledown$ ).

needed to confirm this result in humans.

Puerarin is a flavonoid derivative in *Radix puerariae* (Ge-gen) and is an antagonist of the 5-HT<sub>2C</sub> receptor and benzodiazepine site<sup>[33]</sup>. Puerarin competitively inhibited CYP2D6 in our cell model. There was no relationship between CYP2D6\*1 and \*10 inhibition by puerarin *in vitro*, similar to the *in vivo* experiment previously conducted in our laboratory<sup>[34]</sup>.

In conclusion, we have demonstrated the use of stable CYP2D6 expression cell models in the kinetic assessment of CYP2D6\*1 and \*10-mediated bufuralol 1'-hydroxylation and AMMC-*O*-demethylation. We further investigated CYP2D6 genotype-dependent herb-drug interactions using these cell models. The concentration-dependent inhibition and the representative Eadie-Hofstee plots indicate that these phytochemicals, including bilobalide, coptisine sulfate, schizandrin B, luteolin, schizandrin A, and puerarin competitively inhibit CYP2D6\*1 and \*10 activities. Although CYP2D6\*10 had a lower enzyme activity than CYP2D6\*1, the inhibitions by the phytochemicals were similar between these two variants. Further studies are warranted to identify whether the *in vitro* effects of these phytochemicals have clinical significance in humans.

### Acknowledgements

This work was supported by the State Scholarship Fund from China Scholarship Council (No 201206370103), the National Natural Science Foundation of China (No 81273595, 81072706, and 84402511), the Scientific Foundation of Hunan (No 11K073 and 10JJ4020), the "863" Project (No 2012AA02A518), NCET-10-0843 and the Research Innovation Foundation of Graduate Student in Hunan province, China (CX2011B056). We are grateful to Dr Curtis D KLAASSEN and Helen RENAUD who provided language help.

### Author contribution

Hong-hao ZHOU, Wei ZHANG, and Qiang QU designed the research; Qiang QU, Lu HAN, and Lan-xiang WU performed the research; Yi-wen ZHANG performed HPLC analysis; Jian QU and Min ZHAN analyzed the data; and Qiang QU wrote the paper.

### Abbreviations

AMMC, 3-[2-(*N,N*-diethyl-*N*-methyl-ammonium)ethyl]-7-methoxy-4-methylcoumarin; P450, human cytochrome P450; CYP2D6, human cytochrome P450 2D6; HPLC, high pressure/performance liquid chromatography; RFU, relative fluorescence units.

### References

- 1 Ingelman-Sundberg M. Genetic polymorphisms of cytochrome P450 2D6 (CYP2D6): clinical consequences, evolutionary aspects and functional diversity. *Pharmacogenomics J* 2005; 5: 6–13.
- 2 Backlund M, Ingelman-Sundberg M. Regulation of aryl hydrocarbon receptor signal transduction by protein tyrosine kinases. *Cell Signal* 2005; 17: 39–48.
- 3 Thuerauf N, Lunkenheimer J. The impact of the CYP2D6-polymorphism on dose recommendations for current antidepressants. *Eur Arch Psychiatry Clin Neurosci* 2006; 256: 287–93.
- 4 Bradford LD. CYP2D6 allele frequency in European Caucasians, Asians, Africans and their descendants. *Pharmacogenomics* 2002; 3: 229–43.
- 5 Fukuda T, Nishida Y, Imaoka S, Hiroi T, Naohara M, Funae Y, et al. The decreased *in vivo* clearance of CYP2D6 substrates by CYP2D6\*10 might be caused not only by the low-expression but also by low affinity of CYP2D6. *Arch Biochem Biophys* 2000; 380: 303–8.
- 6 Fugh-Berman A, Ernst E. Herb-drug interactions: review and assessment of report reliability. *Br J Clin Pharmacol* 2001; 52: 587–95.
- 7 Subehan, Usia T, Iwata H, Kadota S, Tezuka Y. Mechanism-based inhibition of CYP3A4 and CYP2D6 by Indonesian medicinal plants. *J Ethnopharmacol* 2006; 105: 449–55.
- 8 Gurley BJ, Gardner SF, Hubbard MA, Williams DK, Gentry WB, Khan IA, et al. *In vivo* effects of goldenseal, kava kava, black cohosh, and valerian on human cytochrome P450 1A2, 2D6, 2E1, and 3A4/5 phenotypes. *Clin Pharmacol Ther* 2005; 77: 415–26.
- 9 Pan Y, Abd-Rashid BA, Ismail Z, Ismail R, Mak JW, Pook PC, et al. *In vitro* effects of active constituents and extracts of *Orthosiphon stamineus* on the activities of three major human cDNA-expressed cytochrome P450 enzymes. *Chem Biol Interact* 2011; 190: 1–8.
- 10 Han YL, Yu HL, Li D, Meng XL, Zhou ZY, Yu Q, et al. *In vitro* inhibition of Huanglian [*Rhizoma coptidis* (L.)] and its six active alkaloids on six cytochrome P450 isoforms in human liver microsomes. *Phytother Res* 2011; 25: 1660–5.
- 11 Chatterjee P, Franklin MR. Human cytochrome p450 inhibition and metabolic-intermediate complex formation by goldenseal extract and its methylenedioxyphenyl components. *Drug Metab Dispos* 2003; 31: 1391–7.
- 12 Ito K, Iwatsubo T, Kanamitsu S, Ueda K, Suzuki H, Sugiyama Y. Prediction of pharmacokinetic alterations caused by drug-drug interactions: metabolic interaction in the liver. *Pharmacol Rev* 1998; 50: 387–412.
- 13 Sawada M, Kamataki T. Genetically engineered cells stably expressing cytochrome P450 and their application to mutagen assays. *Mutat Res* 1998; 411: 19–43.
- 14 Chauret N, Dobbs B, Lackman RL, Bateman K, Nicoll-Griffith DA, Stresser DM, et al. The use of 3-[2-(*N,N*-diethyl-*N*-methylammonium)ethyl]-7-methoxy-4-methylcoumarin (AMMC) as a specific CYP2D6 probe in human liver microsomes. *Drug Metab Dispos* 2001; 29: 1196–200.
- 15 Zhuge J, Yu YN, Wu XD. Stable expression of human cytochrome P450 2D6\*10 in HepG2 cells. *World J Gastroenterol* 2004; 10: 234–7.
- 16 Donato MT, Jiménez N, Castell JV, Gómez-Lechón MJ. Fluorescence-based assays for screening nine cytochrome P450 (P450) activities in intact cells expressing individual human P450 enzymes. *Drug Metab Dispos* 2004; 32: 699–706.
- 17 Livak KJ, Schmittgen TD. Analysis of relative gene expression data using real-time quantitative PCR and the 2(-Delta Delta C(T)) Method. *Methods* 2001; 25: 402–8.
- 18 Beverage JN, Sissung TM, Sion AM, Danesi R, Figg WD. CYP2D6 polymorphisms and the impact on tamoxifen therapy. *J Pharm Sci* 2007; 96: 2224–31.
- 19 Niwa T, Hiroi T, Tsuzuki D, Yamamoto S, Narimatsu S, Fukuda T, et al. Effect of genetic polymorphism on the metabolism of endogenous neuroactive substances, progesterone and p-tyramine, catalyzed by CYP2D6. *Brain Res Mol Brain Res* 2004; 129: 117–23.
- 20 Shen H, He MM, Liu H, Wrighton SA, Wang L, Guo B, et al. Comparative metabolic capabilities and inhibitory profiles of CYP2D6.1, CYP2D6.10, and CYP2D6.17. *Drug Metab Dispos* 2007; 35: 1292–300.

- 21 Defeudis FV. Bilobalide and neuroprotection. *Pharmacol Res* 2002; 46: 565–8.
- 22 Zou L, Harkey MR, Henderson GL. Effects of herbal components on cDNA-expressed cytochrome P450 enzyme catalytic activity. *Life Sci* 2002; 71: 1579–89.
- 23 Woelkart K, Feizlmayr E, Dittrich P, Beubler E, Pini F, Suter A, *et al*. Pharmacokinetics of bilobalide, ginkgolide A and B after administration of three different *Ginkgo biloba* L. preparations in humans. *Phytother Res* 2010; 24: 445–50.
- 24 Gong LL, Fang LH, Wang SB, Sun JL, Qin HL, Li XX, *et al*. Coptisine exert cardioprotective effect through anti-oxidative and inhibition of RhoA/Rho kinase pathway on isoproterenol-induced myocardial infarction in rats. *Atherosclerosis* 2012; 222: 50–8.
- 25 Pao TT, Hsu KF, Liu KT, Chang LG, Chuang CH, Sung CY. Protective action of schizandrin B on hepatic injury in mice. *Chin Med J (Engl)* 1977; 3: 173–9.
- 26 Liu KT, Lesca P. Pharmacological properties of dibenzo[a,c]cyclo-octene derivatives isolated from *Fructus Schizandrae chinensis*. I. Interaction with rat liver cytochrome P-450 and inhibition of xenobiotic metabolism and mutagenicity. *Chem Biol Interact* 1982; 39: 301–4.
- 27 Iwata H, Tezuka Y, Kadota S, Hiratsuka A, Watabe T. Identification and characterization of potent CYP3A4 inhibitors in *Schisandra* fruit extract. *Drug Metab Dispos* 2004; 32: 1351–8.
- 28 Li WL, Xin HW, Su MW, Xiong L. Inhibitory effects of schisandrin A and schisandrin B on CYP3A activity. *Methods Find Exp Clin Pharmacol* 2010; 32: 163–9.
- 29 Zhang YC, Gan FF, Shelar SB, Ng KY, Chew EH. Antioxidant and Nrf2 inducing activities of luteolin, a flavonoid constituent in *Ilexis sonchifolia* Hance, provide neuroprotective effects against ischemia-induced cellular injury. *Food Chem Toxicol* 2013; 59: 272–80.
- 30 Kao TK, Ou YC, Lin SY, Pan HC, Song PJ, Raung SL, *et al*. Luteolin inhibits cytokine expression in endotoxin/cytokine-stimulated microglia. *J Nutr Biochem* 2011; 22: 612–24.
- 31 Foti RS, Wahlstrom JL, Wienkers LC. The *in vitro* drug interaction potential of dietary supplements containing multiple herbal components. *Drug Metab Dispos* 2007; 35: 185–8.
- 32 Shimoi K, Okada H, Furugori M, Goda T, Takase S, Suzuki M, *et al*. Intestinal absorption of luteolin and luteolin 7-O-beta-glucoside in rats and humans. *FEBS Lett* 1998; 438: 220–4.
- 33 Overstreet DH, Kralic JE, Morrow AL, Ma ZZ, Zhang YW, Lee DY. NPI-031G (puerarin) reduces anxiogenic effects of alcohol withdrawal or benzodiazepine inverse or 5-HT<sub>2C</sub> agonists. *Pharmacol Biochem Behav* 2003; 75: 619–5.
- 34 Zheng J, Chen B, Jiang B, Zeng L, Tang ZR, Fan L, *et al*. The effects of puerarin on CYP2D6 and CYP1A2 activities *in vivo*. *Arch Pharm Res* 2010; 33: 243–6.